N-LINKED GLYCOSYLATION REGULATES HUMAN PROTEINASE-ACTIVATED RECEPTOR-1 CELL SURFACE EXPRESSION AND DISARMING VIA NEUTROPHIL PROTEINASES AND THERMOLYSIN

Yu Pei Xiao, Alyn H Morice, Steven J Compton, Laura Sadofsky *
Division of Cardiovascular & Respiratory Studies, University of Hull, Hull York Medical School, East Yorkshire, HU16 5JQ, UK.

Running Head: *N*-linked glycosylation regulates PAR_1 proteinase disarming

*Corresponding Author: Laura Sadofsky. Email: L.R.Sadofsky@Hull.ac.uk

Proteinase-activated receptor 1 (PAR_1) induces activation of platelet and vascular cells after proteolytic cleavage of its extracellular amino terminus by thrombin. In pathological situations, other proteinases may be generated in the circulation and might modify the responses of PAR_1 by cleaving extracellular domains. In this study, epitope-tagged wild-type $hPAR_1$ and a panel of *N*-linked glycosylation-deficient mutant receptors were permanently expressed in epithelial cells (KNRK and CHO cells). We have analysed the role of *N*-linked glycosylation in regulating proteinase activation/ disarming and cell global expression of $hPAR_1$. We reported for the first time that glycosylation in the N-terminus of $hPAR_1$ downstream of the tethered ligand (especially Asn^{75}) governs receptor disarming to trypsin, thermolysin, and the neutrophil proteinases elastase and proteinase 3, but not cathepsin G. In addition, $hPAR_1$ is heavily *N*-linked glycosylated and sialylated in epithelial cell lines, and glycosylation occurs at all five consensus sites, namely, Asn^{35}, Asn^{62}, Asn^{75}, Asn^{250}, and Asn^{259}. Removing these *N*-linked glycosylation sequons effected $hPAR_1$ cell surface expression to varying degrees, and *N*-linked glycosylation at ECL2 (especially Asn^{250}) of $hPAR_1$ is essential for optimal receptor cell surface expression and receptor stability.

Proteinases can exert many biological effects on cells by virtue of their ability to cleave a plethora of protein substrates. Our understanding of proteinase signalling has advanced since the discovery of a small family of G-protein coupled receptors termed proteinase-activated receptors or PAR (1-3). Classically, thrombin activates PAR_1 by proteolytic cleavage of the PAR_1 N-terminal domain between Arg^{41} and Ser^{42} to expose a new N-terminus that acts as a tethered-ligand and subsequently triggers receptor activation (2). Thrombin is a serine proteinase generated at the sites of vascular injury during the coagulation cascade and activates various types of cells in the vasculature like platelets and endothelial cells (2,3). In addition to thrombin, other proteinases may be generated in the circulation under pathological situations, any proteinase that cleaves the correct peptide bond within the N-terminus of PAR_1 may be able to expose the tethered ligand and then initiate intracellular signalling to provoke a cellular response (1,2,4-8). Conversely, proteinases can also disarm PAR_1 by proteolytic removal of the tethered ligand domain from the receptor (4,9-14). Such disarmed receptors remain at the cell surface but are no longer available for activation by activating proteinases (e.g. thrombin), they can however be activated by the corresponding PAR_1-APs (1,2,15). Moreover, some of those proteinases (e.g. trypsin, neutrophil proteinases) have been reported to both activate and/or disarm PAR_1 in different cell systems (2,4,8,13,14,16-18). Activation and desensitization of PAR_1 must be well-controlled in order to eliminate the potential pathological damage resulted from unchecked receptor signalling (14).

Our previous pharmacological studies have reported that activation of $hPAR_2$ by mast cell tryptase can be regulated by receptor N-terminal glycosylation (19,20). To our knowledge, $hPAR_1$ contains a total of five predicted sites for *N*-linked glycosylation, three sequons are located on the receptor N-terminus ($N^{35}A^{36}T^{37}$, $N^{62}E^{63}S^{64}$, and $N^{75}K^{76}S^{77}$) and two are located within extracellular loop 2 (ECL2; $N^{250}I^{251}T^{254}$, and $N^{259}E^{260}T^{261}$) (Fig. 1) (21). PAR_1, downstream of the tethered ligand,

possesses two N-linked glycosylation sequons (Asn^{62} and Asn^{75}) which are located along the N-terminus in a domain where disarming proteinases may target. In addition, previous studies demonstrated that thermolysin and neutrophil proteinases target specific sites which are close proximally to these glycosylation sequons (Fig. 1) (12,13,16). Hence, we have analysed the role of *N*-linked glycosylation in regulating cell surface expression and proteinase activation/disarming of $hPAR_1$. We have permanently expressed epitope-tagged wild-type or glycosylation-deficient mutant $hPAR_1$ in KNRK and CHO (Pro5 and Lec2) cell lines and sought to determine: (i) the influence of *N*-linked glycosylation sequons on the receptor cell surface expression and signalling, and (ii) the role of N-terminal glycosylation sequon, especially Asn^{62} and Asn^{75}, in regulating receptor signalling by neutrophil proteinases and thermolysin.

Experimental Procedure

Materials- DMEM, sodium pyruvate, penicillin, streptomycin, amphotericin B, heat inactivated FCS, non-enzymic cell dissociation solution, geneticin (G418), Opti-MEM media and Lipofectamine 2000, dNTPs and $Oligo(dT)_{12-18}$ primer, Accuprime DNA polymerase, Fluo-3 acetoxymethyl ester were all purchased from Invitrogen Life Technologies Inc. (Paisley, UK). Primers were designed "in-house" and purchased from MWG-biotech (Ebersberg, Germany). PCR purification kits, Gel extraction kits, and plasmid isolation kits were all bought from Qiagen (Crawley, West Sussex, UK). XL1-Blue supercompetent cells and the QuikChange® Site-Directed Mutagenesis Kit were purchased from Stratagene® Europe (Amsterdam, NL). The rapid DNA ligation kit was bought from Roche (Lewes, East Sussex, UK). All restriction enzymes were purchased from New England Biolabs (Hitchin, Hertfordshire, UK). Anti-PAR_1 ATAP-2 monoclonal antibody was purchased from Zymed Laboratories Inc. (San Francisco, USA). PAR_1-APs $TFLLR\text{-}NH_2$ was purchased from Peptides International (Kentucky, USA). Enhanced yellow fluorescent protein (eYFP) was obtained from BD Biosciences Clontech (Alto, USA). Proteinase 3 was obtained from Athens Research & Technology (Athens Research & Technology, Inc. Athens, Greece). Human leukocyte elastase and cathepsin-G were purchased from Elastin Products (Elastin Products Company, Inc. Missouri, USA). M-Per mammalian protein extraction reagent and the ProFound HA.11 immunoprecipitation kit were purchased from PIERCE (PIERCE, Cheshire, UK). All other chemicals and reagents were purchased from Sigma-Aldrich (Poole, Dorset, UK) unless otherwise stated.

Generation of cDNAs encoding wt-$hPAR_1$E- Using an overlapping PCR approach, enhanced yellow fluorescent protein (eYFP) was fused to the C-terminal of wt-$hPAR_1$ (POMC-M1-$hPAR_1$-HA.11 in pcDNA3.1: C-terminally tagged with an HA.11 epitope and N-terminally tagged with an M1 epitope and a Pro-opiomelanocortin (POMC)) to generate wt-$hPAR_1$E (POMC-M1-$hPAR_1$-HA.11-eYFP). The wt-$hPAR_1$E was subsequently amplified and purified, and then sequenced by MWG.

Generation of glycosylation-deficient mutant cell lines- All glycosylation-deficient mutants were generated using the QuickChange® site-directed mutagenesis kit and confirmed by MWG sequencing. The oligonucleotides were designed to replace the asparagine (N) residues at positions Asn^{35}, Asn^{62}, Asn^{75}, Asn^{250}, and Asn^{259} with glutamine (Q) residues. Single-site mutants (N35Q, N62Q, N75Q, N250Q, and N259Q) were first constructed. In order to elucidate the cumulative effects of a lack of glycosylation at multiple sites, four receptors with multiple glycosylation mutations (N62QN75Q, N35QN62QN75Q, N250QN259Q, and N35-259Q) were constructed. In addition, the alanine (A) mutations were created at amino acid position Phe^{55}-Trp^{56} or Val^{72}-Ser^{73} of N62QN75Q to generate cathepsin G mutant (F55AW56A) or proteinase 3 mutant (V72AS73A). KNRK and CHO cells permanently expressing wild type or mutant $hPAR_1$ cell lines were generated and cultured as previously described (Table 1) (19,20).

Flow Cytometry Analysis (FACs)- WT and mutant cells lines (approx. 90% confluence) with matched receptor expression were selected and used for further studies by

FACs (Becton Dickinson, Franklin Lakes, NJ, U.S.A.) as we previously described (19). The anti-PAR_1 ATAP-2 monoclonal antibody (1µg/ml) and anti-mouse FITC-conjugated antibody (1 in 1000 dilution) were applied to assess the levels of receptor cell-surface expression. The data was expressed as the median fluorescence of positive minus the median fluorescence of the EV (pcDNA3.1 transfected KNRK) cells.

Confocal Microscopy Analysis- For the wt-$hPAR_1$eYFP and mutant cell lines, the light emitted by the eYFP (530 nm) fused to the receptor was used to assess receptor expression. Cells on coverslips were fixed by incubation in formaldehyde (3%) in PBS for 15 minutes at RT, and then permeabilised in PBS containing 0.2% triton X-100 for 10 minutes at RT. The coverslips were then mounted with anti-fade and fixed to slides. The cells were visualised by a Nikon Eclipse (TE2000-E) microscope with a BioRad Radiance 2100 scanning system and lasers.

Western Blot Analysis- HA.11 tagged wild type and glycosylation-deficient mutants of $hPAR_1$E were immunoprecipitated using a ProFound HA.11 immunoprecipitation kit as per the manufacturer's protocol. Protein samples (20µg) were separated on a 10% SDS/PAGE gel before transfer to Hybond C PVDF membrane. The membrane was subsequently blocked with PBS containing 5% non-fat milk before incubation overnight at 4°C with the mouse monoclonal HA.11 antibody (1:1000 dilution in PBS/Tween-20 (0.1%) containing 2% non-fat milk). Blots were washed with PBS/Tween 20 (0.1%) for 1 h, replacing the buffer every 15 min, before a final incubation with the peroxidase conjugated goat anti-mouse IgG ([1 in 4000] in PBS/Tween-20 (0.1%) containing 2% non-fat milk) for 1 hour. Following a further wash in PBS/Tween 20 (0.1%) for 1 hour bands were visualized using ECL (Amersham Biosciences, UK).

Calcium Signalling Assay- The calcium signalling assay was performed as we described previously (19). Functional receptor activity was assessed by challenging cells with the PAR_1-AP TFLLR-NH_2 (100 µM) and thrombin (5 nM). To assess whether a test proteinase was amputating the tethered ligand from the receptor (disarming), cells were first challenged by addition of the test proteinase for 2 mins. Successful amputation of the tethered ligand was then monitored by a subsequent application of thrombin (5 nM). The calcium signal in response to thrombin will be ablated if the tethered ligand has been removed from the receptor by the test proteinase. To demonstrate that the disarmed PAR_1 is still functional and present at the cell surface, 100 µM TFLLR-NH_2 was applied after thrombin challenge. A calcium signal triggered by the TFLLR-NH_2 is indicative of a functional PAR_1 at the cell surface, which is unresponsive to thrombin.

Calculations and statistical analysis- Data were analyzed using Prism Graphpad software. Statistical tests were carried out depending on the specifics of the datasets to be compared. When a comparison of two cell lines subjected to the same treatment was compared, a paired student's t test was adopted. The comparison of a group of cell lines subjected to the same treatment was performed by one-way ANOVA followed by Tukey's Multiple Comparison Test. In order to assess the changes over a period of time using a specific treatment or to assess a change over a concentration range between two different cell lines two-way ANOVA tables were adopted.

RESULTS

N-linked Glycosylation at Specific Sites Regulates $hPAR_1$ Cell Surface Expression. Flow cytometry analysis (FACS) demonstrated that removing any of the glycosylation sequons resulted in a significant decrease ($p<0.001$) in $hPAR_1$ cell surface expression in KNRK cells (Fig. 2). N35Q displayed the greatest cell surface expression; N250Q displayed the lowest expression when compared to the other single mutants N35Q, N62Q, N75Q, N250Q and N259Q [percentage relative to WT ± SEM: 55 ± 4 %; 26 ± 3 %; 13 ± 1.5 %; 10.5 ± 0.7 % and 26 ± 3 % (n=3) respectively]. Removal of both glycosylation sequons on ECL2 (N250QN259Q) resulted in near total loss of cell surface expression [percentage relative to WT ± SEM: 6±1 % (n=3)]. In contrast removing all glycosylation sequons on the N-terminus (N35QN62QN75Q) still resulted in nearly 50% cell surface expression compared to WT expression [percentage relative to WT ± SEM: 44.7 ±

1 % (n=3)]. Removing all glycosylation sequons resulted in a receptor (N35-259Q) that was expressed at a similar level to the N250QN259Q mutant [percentage relative to WT ± SEM: 6 ± 1 % (n=3)].

Analysis of eYFP tagged $hPAR_1$ localisation in permeabilized cells by confocal microscopy demonstrated that all $hPAR_1E$ types (wt and glycosylation-deficient mutant $hPAR_1$) with the exception of N35-259Q$hPAR_1E$ were expressed on the cell surface; however, different levels of membrane localisation and cytosolic retention were observed (Fig. 3). There was no detectable fluorescence (eYFP signalling) observed in EV cells (Fig. 3A). Wt-$hPAR_1E$ displayed strong cell membrane expression with little receptor observed in the cytoplasm (Fig. 3B). Removal of sequon Asn^{35} in the receptor N-terminus resulted in the appearance of receptor within the cytosol (Fig. 3C). Removal of both sequons (Asn^{62} and Asn^{75}) after the tethered ligand of $hPAR_1$ resulted in a large amount of receptor being found in the cytosol (Fig. 3D). The relative intensity of the receptor membrane localisation and global cellular distribution appeared to be reduced significantly after removal of ECL2 glycosylation sequons (Asn^{250} and Asn^{259}) (Fig. 3E). Removal of all $hPAR_1$ glycosylation sequons (Asn^{35}, Asn^{62}, Asn^{75}, Asn^{250} and Asn^{259}) resulted in a dramatic loss of cell surface expression with the highest level of receptor cytosolic retention (Fig. 3 F).

$hPAR_1$ is a Heavily Glycosylated and Sialylated Receptor. All of the glycosylation-deficient mutant receptors displayed different degrees of loss in molecular mass; no bands were detected in EV cells (Fig. 4A). The molecular mass of WT-$hPAR_1E$ migrated as a broad band ranging from ~37 kDa to ~250 kDa, with the majority of the receptor being observed from ~75 kDa to ~220 kDa. This is a similar pattern to that of N62Q$hPAR_1E$. N62QN75Q$hPAR_1E$ migrated from ~37 kDa to ~120 kDa. N35QN62QN75Q$hPAR_1E$ migrated with a molecular mass from ~37 kDa to ~200 kDa, with the majority of the receptor being observed from ~75 kDa to ~120 kDa. The predicted molecular mass of the fused $hPAR_1$eYFP is approximately ~70kDa to ~80 kDa ($hPAR_1$ is ~47 kDa and eYFP protein is ~31 kDa). We proposed that the band at ~75 kDa may represent an unglycosylated monomer of PAR_1; the bands around ~80kDa to ~130 kDa may represent a glycosylated monomer of PAR_1; and the bands around ~150kDa to ~220 kDa may represent glycosylated and unglycosylated dimers of PAR_1 (Fig. 4). When removing all three glycosylation sites (Asn^{35}, Asn^{62}, Asn^{75}) in the N-terminus of the receptor, the banding pattern changed with only glycosylated dimer and unglycosylated monomer present. Removal of glycosylation at sites Asn^{62} and Asn^{75} produced a single band at ~120 kDa representing a glycosylated monomer of PAR_1. Only one band migrated at ~37 kDa from both N250QN259Q$hPAR_1E$ and N35-259Q$hPAR_1E$. A number of minor bands that may represent either eYFP protein or proteolytic degradation products of $hPAR_1$ were routinely observed around ~37 kDa in all lanes.

To determine the contribution of sialic acid to the molecular mass of $hPAR_1$, we performed western blot analysis for wt-$hPAR_1E$ transfected CHO cells (Pro5 and Lec2) (Fig. 4B). No bands were detected in the non-transfected Lec2 and Pro5. Pro5-PAR_1E migrated as broad high molecular weight band ranging from ~25 kDa to ~200 kDa; the molecular mass of Lec2-PAR_1E ranged from ~25 kDa to ~150 kDa. Two bands were routinely observed between the ~25 kDa to ~37 kDa ranges in both of Pro5-PAR_1E and Lec2-PAR_1E.

The N-linked Glycosylation Located After the Tethered Ligand of $hPAR_1$ Regulates $hPAR_1$ Signalling. To investigate whether *N*-linked glycosylation at individual residues had a role in regulating receptor function, we constructed calcium signalling concentration-effect curves for thrombin, trypsin and TFLLR-NH_2, in wt-$hPAR_1$ and $hPAR_1$ glycosylation mutant KNRK cell lines. The EC_{50} values of wt-$hPAR_1$ and mutant receptors for the calcium signalling assay are displayed in Table 2.

N62QN75Q concentration effect curves were compared with WT-M since they displayed similar cell surface expression ($p>0.05$) (Fig. 5A). TFLLR-NH_2 displayed a slight rightward shift in activating N62QN75Q compared with WT-M, stimulating a calcium signal at 3-100 µM for WT-M and 10-100 µM for N62QN75Q

respectively, but achieved the same maximum response of 42 ± 1.5% of A23187 at 100 μM in both cell lines (Fig. 5B). For N62QN75Q and WT-M, thrombin induced a calcium signal from 0.05 nM to 5 nM (Fig. 5C). However, the magnitude of the responses to thrombin in N62QN75Q was smaller than those obtained for WT-M (24 ± 2.6 % of A23187 and 31 ± 1.8 % of A23187 respectively) ($p>0.05$). The EC_{50} value for thrombin in N62QN75Q was 0.3 nM and for WT-M was 0.12 nM. Interestingly, the N62QN75Q displayed reduced sensitivity towards trypsin compared to WT-M, and the maximal response achieved was only 14% of A23187 compared to 32 ± 3 % of A23187 for the WT-M ($p<0.001$) (Fig. 5D). In addition, the EC_{50} value for trypsin in N62QN75Q was significantly greater than WT-M (42 nM and 26 nM respectively).

However, further analysis of N62Q and N75Q cell lines, revealed no observable changes in receptor function for TFLLR-NH2, thrombin or trypsin when compared with their matched wt-$hPAR_1$ cell line (data not shown).

Removal of N-linked Glycosylation Asn^{62} and/or Asn^{75} from $hPAR_1$ Enhances the Ability of Trypsin to Disarm the Receptor. Having found that trypsin shows reduced activity towards N62QN75Q by calcium signalling assay, we then explored the ability of trypsin to disarm N62QN75Q, N62Q and N75Q.

Fig. 6A shows the TFLLR-NH_2 (100 μM) responses following trypsin (3, 10, 30, 100, 300 nM) and then thrombin (5 nM) challenge in WT-M and N62QN75Q cells (i.e. trypsin then thrombin and then TFLLR-NH_2). For WT-M the TFLLR-NH_2 responses remained the same after challenging the cells with trypsin from 3-300 nM. Challenging the N62QN75Q cells with 3 nM trypsin followed by 5 nM thrombin, and then 100 μM TFLLR-NH_2, triggered a calcium signal that was similar to that seen for WT-M cells. However, a robust increase in the magnitude of TFLLR-NH_2 triggered calcium signal was observed after challenging the N62QN75Q cells with 300 nM trypsin, which was over 4-fold greater than that observed for WT-M cells ($p<0.05$).

We next assessed whether individual glycosylation at Asn^{62} or Asn^{75} is responsible for regulating trypsin disarming of $hPAR_1$ (Fig. 6B & C). Challenging N62Q cells with 5 nM thrombin or 100 μM TFLLR-NH_2 resulted in a calcium response of 61.4 ± 6.7 % of A23187 and 62 ± 6.9 % of A23187 respectively (Fig. 6B). Challenging N62Q cells with 100 nM trypsin resulted in an observable calcium signal (32 ± 8 % of A23187). Addition of thrombin following trypsin challenge resulted in a marked reduction ($p< 0.001$) in the calcium response to thrombin compared with the response obtained with thrombin added alone (7.8 ± 1 % of A23187 *vs.* 61.4 ± 6.7 % of A23187). Addition of TFLLR-NH_2 following trypsin and thrombin resulted in a response that was slightly increased ($p>0.05$) in magnitude compared to the response obtained to TFLLR-NH_2 following just thrombin addition (17.5 ± 3.6 % of A23187 *vs.* 9 ± 3 % of A23187), but was significantly reduced ($p< 0.001$) compared with the response of TFLLR-NH_2 added alone (17.5 ± 3.6 % of A23187 *vs.* 62 ± 6.9 % of A23187).

Challenging N75Q cells with trypsin only resulted in a response 8 ± 1 % of A23187 (Fig. 6C). Challenging N75Q cells with TFLLR-NH_2 or thrombin alone resulted in a calcium response of 27 ± 2 % of A23187 and 12 ± 0.7 % of A23187 respectively. Addition of TFLLR-NH_2 following thrombin addition resulted in a calcium response 12 ± 1.7 % of A23187. Addition of thrombin following addition of trypsin resulted in no calcium response. Finally, challenging the cells with TFLLR-NH_2 following trypsin and thrombin addition triggered a calcium response 21 ± 2.7 % of A23187, which was of comparable ($p>0.05$) magnitude to the response obtained with TFLLR-NH_2 alone.

Elastase, Proteinase 3 and Thermolysin, but not Cathepsin G Displayed Enhanced Ability to Disarm $hPAR_1$(N62QN75Q). Effective proteinase receptor disarming was assessed by thrombin activation of the cells following proteinase addition. For N62QN75Q and WT-M significant differences ($p< 0.0001$) in responses to 5 nM thrombin following the addition of elastase at different concentrations were observed (Fig. 7A). For WT-M no changes were observed in thrombin triggered calcium responses after the addition of 1 nM elastase, and the

thrombin triggered calcium response was totally ablated after addition of 15 nM elastase. The thrombin response curve for N62QN75Q shifted left half a log when compared to WT-M. For N62QN75Q the calcium signalling response to thrombin started to decrease after challenging the cells with 1 nM elastase (~80% of control Thrombin response). The thrombin triggered calcium response was totally ablated after challenging cells with 5 nM elastase.

For N62QN75Q and WT-M no significant differences ($p>0.05$) in responses to 5 nM thrombin following the addition of cathepsin G from 10 nM to 300 nM were observed (Fig. 7B). The thrombin triggered calcium response was totally ablated after addition of 300 nM cathepsin G for both N62QN75Q and WT-M.

For N62QN75Q and WT-M significant differences ($p< 0.0001$) in responses to 5 nM thrombin following the addition of proteinase 3 were observed (Fig. 7C). For WT-M no changes were observed in the thrombin triggered calcium response following the addition of 1000 nM proteinase 3. In contrast, significant decreases in the response to thrombin were observed in N62QN75Q following the addition of proteinase 3 from 1 nM to 1000 nM. The thrombin triggered calcium signal was totally abolished after the addition of 1000 nM proteinase 3.

For N62QN75Q and WT-M significant differences ($p< 0.0001$) in responses to 5 nM thrombin following the addition of thermolysin at different concentrations were observed (Fig. 7D). The thrombin response curve after adding thermolysin at increasing concentration for N62QN75Q shifted 30-fold to the left when compared to WT-M. For N62QN75Q the calcium signalling response to thrombin started to decrease after application of thermolysin at 3 nM (~80% of control thrombin response). The thrombin triggered calcium response was totally ablated after challenging N62QN75Q with 300 nM thermolysin. However, for WT-M the thrombin triggered calcium responses remained elevated at thermolysin concentrations up to 30 nM. The calcium signalling response to thrombin started to decrease following 100 nM thermolysin addition (~80% of thrombin control). The thrombin triggered calcium response in WT-M was totally ablated after addition of 1000 nM thermolysin.

Molecular Evidence that Cathepsin G and Proteinase 3 are Disarming $hPAR_1(N62QN75Q)$. Addition of 100 nM cathepsin G to N62QN75Q cells before the addition of 5 nM thrombin markedly reduced ($p< 0.001$) the response to thrombin compared with the response obtained with thrombin added alone (11 ± 2 % of A23187 and 30 ± 5 % of A23187 respectively) (Fig. 8A). In contrast, prior addition of cathepsin G failed to reduce the thrombin calcium signal in cathepsin G mutant cells when compared to the control (32.5 ± 8 % of A23187 and 36.5 ± 8 % of A23187 respectively) ($p>0.05$).

No observable calcium response to thrombin was observed when 300 nM proteinase 3 had been added to the N62QN75Q cells prior to thrombin challenge (Fig. 8B). In contrast, prior addition of proteinase 3 failed to reduce the thrombin calcium signal in the proteinase 3 mutant cells, when compared to the response obtained with thrombin added alone (13 ± 2 % of A23187 and 12.33 ± 2.5 % of A23187 respectively) ($p>0.05$) .

Elastase, Cathepsin G, Proteinase 3 and Thermolysin Mainly Disarm $hPAR_1(N75Q)$. The ability of thermolysin and neutrophil serine proteinases to activate/disarm N62Q and N75Q was investigated (Fig. 9).

Challenging N62Q cells with 5 nM thrombin or 100 µM TFLLR-NH_2 resulted in a calcium response of 64.7 ± 7 % of A23187 and 67.8 ± 5 % of A23187 respectively (Fig. 9A). In addition, challenge with TFLLR-NH_2 following thrombin addition resulted in a calcium response of 9 ± 3 % of A23187. Thermolysin (50 nM) had no observable effect on calcium signalling in N62Q. Challenge with thrombin following thermolysin addition resulted in a calcium response at 53.5 ± 4.6% of A23187 which is comparable to that obtained with thrombin added alone (64.7 ± 7 % of A23187). Addition of TFLLR-NH_2 following thermolysin and thrombin resulted in a similar calcium response to the response obtained with TFLLR-NH_2 following just thrombin challenge (13.6 ± 4 % of A23187 and 9 ± 3 % of A23187 respectively). Addition of 1.5 nM elastase had no

observable effect on calcium signalling in N62Q cells. Addition of thrombin following elastase addition resulted in a calcium response 49 ± 3.5 % of A23187. Addition of TFLLR-NH_2 following the disarming with elastase and thrombin resulted in a similar calcium response to the TFLLR-NH_2 response obtained following just thrombin alone 12 ± 1 % of A23187 and 9 ± 3 % of A23187 respectively). Addition of 100 nM cathepsin G had no observable effect on calcium signalling in N62Q cells. After challenging N62Q cells with cathepsin G, addition of thrombin resulted in a small decrease in the calcium response compared to that obtained with thrombin added alone (39 ± 3.8 % of A23187 and 64.7 ± 7 % of A23187 respectively). Addition of TFLLR-NH_2 following the addition of thermolysin and thrombin triggered a calcium response at 16 ± 6 % of A23187 that was slightly larger than that obtained with TFLLR-NH_2 following thrombin alone (9 ± 3 % of A23187). Addition of 300 nM proteinase 3 had no observable effect on calcium signalling in N62Q cells. Challenge with thrombin following proteinase 3 addition resulted in a calcium response 67 ± 6.7 % of A23187 which is comparable to that obtained when thrombin was added alone (64.7 ± 7 % of A23187). Addition of TFLLR-NH_2 following the addition of proteinase 3 and thrombin resulted in a calcium response similar to that obtained with TFLLR-NH_2 following thrombin addition (11.6 ± 4 % of A23187 and 9 ± 3 % of A23187 respectively).

Challenging N75Q cells with thrombin or TFLLR-NH_2 resulted in a calcium response 12 ± 0.7 % of A23187 and 27 ± 2 % of A23187 respectively. Addition of TFLLR-NH_2 following thrombin challenge resulted in a calcium response 13.6 ± 1 % of A23187 (Fig. 9B). No observable calcium response was detected after challenging N75Q cells with thermolysin. After challenging N75Q cells with thermolysin, addition of thrombin resulted in a calcium response which was comparable to that obtained to thrombin alone (10 ± 1 % of A23187 and 12 ± 0.7 % of A23187 respectively), and finally challenging the cells with TFLLR-NH_2 triggered a calcium response 21 ± 2 % of A23187. No observable calcium response was detected after challenging N75Q cells with elastase or with thrombin following the addition of elastase. In addition, the response to TFLLR-NH_2 following elastase and thrombin challenge was the same as that obtained with TFLLR-NH_2 alone (28 ± 1 % of A23187 *vs.* 27 ± 2 % of A23187).

Addition of cathepsin G had no observable effect on calcium signalling in N75Q cells. Challenging cells with thrombin following the addition of cathepsin G resulted in a calcium response 10 ± 1 % of A23187 which was comparable to that obtained with thrombin alone (12 ± 0.7 % of A23187). Addition of TFLLR-NH_2 following the addition of cathepsin G and thrombin triggered a calcium response, which was of similar magnitude to that obtained with TFLLR-NH_2 following thrombin alone (17 ± 1 % and 13.6 ± 1 % of A23187 respectively). Addition of proteinase 3 had no observable effect on calcium signalling in N75Q cells. Addition of thrombin after challenging N75Q cells with proteinase 3 resulted in a very small decrease in calcium response compared to that obtained with thrombin alone (10 ± 0.5 % of A23187 and 12 ± 0.7 % of A23187 respectively). Finally challenging the cells with TFLLR-NH_2 following proteinase 3 and Thrombin addition triggered a calcium response 20.5 ± 0.5 % of A23187.

DISCUSSION

In the present study, we have demonstrated for the first time that *N*-linked glycans (Asn^{62} and Asn^{75}) after the tethered ligand on the N-terminus of $hPAR_1$ regulate receptor signalling to trypsin, thermolysin and the neutrophil proteinases elastase and proteinase 3, but not cathepsin G. In addition, we reported that $hPAR_1$ is heavily *N*-linked glycosylated and sialylated in epithelial cell lines (KNRK and Pro5 cells), and glycosylation occurs at all five consensus sites, namely, Asn^{35}, Asn^{62}, Asn^{75}, Asn^{250}, and Asn^{259}. Removing *N*-linked glycosylation sequons at these positions affected $hPAR_1$ cell surface expression to varying degrees, and *N*-linked glycosylation at ECL2 (especially Asn^{250}) of $hPAR_1$ might be essential for optimal receptor cell surface expression and receptor stability.

N-linked glycosylation, which adds oligosaccharides to the nitrogen in the side-chain amide of asparagines residues, requires the asparagines in a consensus sequence of Asn-X-Ser/Thr (where X is any amino acid except proline) (22,23). However, not all consensus sites are actually glycosylated as the oligosaccharide might be trimmed and elaborated during transit through the endoplasmic reticulum (ER) and the Golgi apparatus (23). Disrupting the glycosylation sites by mutagenesis, individually and/or in combination, allowed us to investigate the status and even the function of each specific putative *N*-linked glycosylation site.

We first examined the role of *N*-linked glycosylation in regulating the receptor cell surface expression and the receptor global distribution in KNRK cells. Interestingly unlike previous studies in HeLa (24), there is still a very high level of cell surface expression of $hPAR_1$ when removing all glycosylation sites on the N-terminus. The ECL2 single glycosylation mutant N250Q displayed the lowest level of cell surface expression of $hPAR_1$ among all the other single glycosylation mutants; furthermore, removing all glycosylation sequons on ECL2 resulted in similar low levels of receptor cell surface expression to the non-glycosylation mutant where all glycosylation sequons had been deleted. *N*-linked glycosylation of $hPAR_1$ on ECL2 (especially Asn^{250}) versus glycosylation in the N-terminus might therefore be more important for receptor optimal cell surface expression. Glycosylation on ECL2 of PAR_2 is also important for enhancing receptor expression but not regulating receptor signalling; more importantly the ECL2 region is extremely sensitive to mutations and mutating residues in and around the glycosylation sequon, even neutral mutations such as alanine (Ala) in ECL2 glycosylation sequon alters receptor structure and function (19,24). The PAR_1 glycosylation study on HeLa cells reported that N-terminal *N*-linked glycosylation of PAR_1 versus ECL2 *N*-linked glycosylation are critical for the regulation of PAR_1 signalling and trafficking (24). In this study, mutants were generated by substituting alanine (Ala) for glutamine (Glu). It is therefore hard to determine whether the altered $hPAR_1$ cell surface expression and signalling in HeLa cells is as a result of the loss of *N*-linked glycosylation or due to the Ala substitution altering receptor structure and function. We have generated our *N*-linked glycosylation mutants by substituting asparagine (Asn) for glutamine (Glu) at all five potential *N*-linked glycosylation sites, Glu is chemically and structurally more similar to Asn. For this reason, we propose that this substitution itself will not lead to structural and functional differences between the mutants and wild-type $hPAR_1$, and any differences detected should be due to the loss of glycosylation.

Using confocal microscopy we demonstrated that the glycosylation-deficient mutants, were abundant in the cytosol. Removal of a single N-terminal glycan resulted in observable receptor cytosolic retention, but removal of all glycosylation sites produced a receptor which could mainly be seen in the cytosol with minimal cell surface expression. Therefore, we conclude that *N*-linked glycosylation of $hPAR_1$ at all sites might be required for the optimal receptor cell surface expression (24,25).

Similar to Soto's study (24), we have demonstrated that in KNRK cells $hPAR_1$ is heavily glycosylated and the glycosylation occurs at all five consensus sites. Removal of *N*-linked glycosylation from ECL2 or removal of all *N*-linked glycans from the receptor resulted in only a single western blot band visualised at around 37kDa compared with wild type or the N-terminus mutants which produced a second band at a lower molecular weight. It is well known that *N*-linked glycosylation can regulate receptor conformation, folding, or stability and even protecting receptors from proteolytic degradation. The bands shown around ~37kDa may represent either eYFP protein or deglycosylation/ or proteolytic degradation products of $hPAR_1$ (5,14,24,26-28). We thus propose that *N*-linked glycosylation especially on ECL2 (Asn^{250} and Asn^{259}) of $hPAR_1$ might be vital for receptor stability and even protecting $hPAR_1$ from endogenous proteolytic degradation. Furthermore, we expressed the $hPAR_1$ in CHO cells (Pro5 and Lec2) in order to assess the sialylation status of $hPAR_1$. The Pro5 cell line is the parent clone for the Lec2 cell line which has a substantial loss in ability to

attach sialic acid to the terminal positions on oligosaccharides. Western blot analysis of $hPAR_1$ in Lec2 cells revealed a protein that had a molecular mass that was up to ~47 kDa lower than that observed for $hPAR_1$ expressed in the Pro5 cells. Presumably this significant loss of ~47 kDa is due to the loss of receptor-associated sialic acid, and we can therefore conclude that $hPAR_1$ in Pro5 cells, at least, is a heavily sialylated receptor.

In order to establish the role of *N*-linked glycosylation on the N-terminus of $hPAR_1$ in regulating receptor function, agonist concentration effect curves were produced for the glycosylation-deficient $hPAR_1$ cell lines and their respective wt-$hPAR_1$ cell line to evaluate the coupling of the mutant receptors to calcium. Receptor cell surface expression for each mutant cell line was compared and matched by FACs to wt-$hPAR_1$ cells in order to ensure any functional differences detected were not due to differences in receptor cell surface expression (19). Except N62QN75Q mutant, no significant changes in receptor function were detected when compared with their respective matching wt-$hPAR_1$ for all mutant cell lines. This N62QN75Q mutant displayed a slight reduction in sensitivity towards lower concentrations of TFLLR-NH_2 and thrombin although statistical analysis showed no significant differences in EC_{50} value and receptor maximum calcium signalling response towards 100 µM TFLLR-NH_2 or 5nM thrombin. The biggest reduction in agonist sensitivity was observed with trypsin activation. PAR_1 coupling to calcium signalling appears not to be affected by the lack of glycosylation on the receptor. Even the N35-259Q mutant cell line still displayed a detectable calcium signal towards TFLLR-NH_2 and thrombin (data not shown); thus adding strength to this conclusion.

In our experiments trypsin triggered calcium signalling in wild-type $hPAR_1$ and its mutants to varying degrees. However, TFLLR-NH_2 calcium signalling response after addition of trypsin and thrombin is much greater in N62QN75Q mutants compared to wild-type $hPAR_1$. This just confirmed that trypsin disarms the mutant receptor, and the disarmed mutant receptors still remained on the cell surface but cannot be activated by thrombin anymore as the tethered ligand has been removed, however, TFLLR will still activate those mutant receptor by binding to receptor ECL2. Trypsin can activate PAR_1 by cleaving at the activating cleavage site Arg^{41}-Ser^{42} to expose the tethered ligand (2,4,29). Moreover, trypsin has also been reported to cleave PAR_1 at residues Arg^{70}-Leu^{71} and Lys^{82}-Gln^{83} which amputates the tethered ligand from the receptor (4) (Fig. 1). Furthermore these residues are suggested to be cleaved by trypsin much faster than the residues Arg^{41}-Ser^{42} (9). Given that these two potential trypsin cleavage sites are located close to Asn^{75}, it is not surprising that in the N62QN75Q and N75Q mutants trypsin can gain easy access to these cleavage sites and therefore disarm these mutant receptors. In contrast, when PAR_1 is fully glycosylated at Asn^{75} these cleavage sites are subsequently shielded by the attached oligosaccharide and thus trypsin disarms wt-$hPAR_1$ less efficiently. Interestingly, Nakayama's previous study reported that 100 nM trypsin cleaved PAR_1 but did not activate it in HUVEC cells, thus suggesting receptor disarming (9). We therefore assume that the glycosylation status of PAR_1 in HUVEC cells must be different to our PAR_1-KNRK system. Indeed, previous studies reported that PAR_1 expressed in HUVECS and platelets migrated as a homogenous species with an apparent mass of 66 kDa (27). This molecular mass is considerably below that reported in other cell systems, including ours, and suggests that PAR_1 is not so heavily glycosylated in these cell types. Therefore we suggest that the Asn^{62} and Asn^{75} might not be fully glycosylated in HUVECs and therefore these potential trypsin cleavage sites around Asn^{75} are more readily available for trypsin cleavage, and subsequent disarms.

We have also shown that the neutrophil proteinases elastase, cathepsin G and proteinase 3 do not activate PAR_1 in our KNRK cell system, but rather disarm the receptor. Like us, Renesto and co-workers reported that elastase, cathepsin G and proteinase 3 can cleave and inactivate PAR_1 in platelets and human endothelial cells (13). In contrast, Suzuki and colleagues reported that elastase can activate PAR_1 in human lung epithelial cells and also mentioned that proteolytic cleavage of PAR_1 by elastase

might activate or inactivate the receptor depending on the site of cleavage (8). The authors also suggested that the extent of glycosylation of the receptor could influence the site and extent of cleavage of the receptor (8).

In our current study, we note that elastase disarms N62QN75Q better than wt-$hPAR_1$ at the same concentration, and 1.5nM elastase disarms N75Q, but not N62Q. Renesto and colleagues' mass spectrometry study indicated that elastase cleaves the N-terminus of $hPAR_1$ at Val^{72}-Ser^{73} and Ile^{74}-Asn^{75} that are located after the tethered ligand (13). Furthermore, Loew *et al.* reported that elastase cleaved the PAR_1 exodomain at Ala^{36}-Thr^{37}, Val^{72}-Ser^{73} and Ala^{86}-Phe^{87} sites with preferential cleavage at Val^{72}, which would disable the receptor (4). Therefore after amputating the Asn^{75} glycosylation, the potential cleavage sites Val^{72}-Ser^{73} might be more easily accessible for elastase cleavage.

Since cathepsin G has been reported to have both activating and disarming actions on PARs (12,13,30,31), we tested the role of N-terminal glycosylation of $hPAR_1$ in regulating this proteinase. We have demonstrated that cathepsin G could clearly disarm N62QN75Q and wt-$hPAR_1$ to the same efficiency. In addition, our data also revealed that cathepsin G at 100 nM disarms N62Q and N75Q. Like us others have also reported that cathepsin G at 30nM could disarm PAR_1 (30). Molino *et al.* reported that in addition to the Arg^{41}-Ser^{42} site, cathepsin G cleaves PAR_1 at Phe^{43}-Leu^{44} and Phe^{55}-Trp^{56} removing the tethered ligand and rendering the receptor unresponsive to thrombin (12). In 1997 Renesto and colleagues' mass spectrometry study indicated that cathepsin G cleaves PAR_1 on platelets and endothelial cells downstream of the thrombin cleavage site at Phe^{55}-Trp^{56} and Tyr^{69}-Arg^{70} (13). Thus we then concluded that cathepsin G might have four potential cleavage sites in the N-terminus of $hPAR_1$ (Arg^{41}-Ser^{42}, Phe^{43}-Leu^{44}, Phe^{55}-Trp^{56}, and Tyr^{69}-Arg^{70}). Furthermore, Loew *et al.* kinetic analyses showed that the preferential cathepsin G cleavage site for PAR_1 is Phe^{55}-Trp^{56} site (4). Moreover, our finding with the cathepsin G mutant is in accord with previous report that has demonstrated that Phe^{55}-Trp^{56} is the main region cleaved within the receptor N-terminus by cathepsin G (12). Also, our western blot data revealed that Asn^{62} is not heavily glycosylated in our KNRK system. Therefore we suggest that cathepsin G sensitivity towards $hPAR_1$ is not regulated by *N*-linked glycosylation.

We have also assessed proteinase 3 inhibition of thrombin-induced Ca^{2+} mobilization in wt-$hPAR_1$, N62QN75Q, N62Q and N75Q. Our data revealed that 300 nM proteinase 3 disarms N62QN75Q but not wt-$hPAR_1$, N62Q or N75Q. It is well established that proteinase 3 has an elastase-like specificity for Ala, Ser, and Val at the P1 site (32). One previous study on human oral epithelial cells also pointed out that proteinase 3 can rapidly cleave PAR_2 between Arg and Ser and relatively inefficiently cleave between Lys and Val (33). Furthermore, proteinase 3 cleaved the peptide corresponding to the N-terminus of PAR_2 at Arg^{36}-Ser^{37} indicating that site of the PAR_2 is structurally accessible by proteinase 3 (33). Interestingly, one previous study on synthetic peptides reported that the cleavage site for proteinase 3 in the N-terminus of PAR_1 is Val^{72}-Ser^{73} (13). In addition, Loew and colleagues' kinetic analysis on the N-terminus domain of PAR_1 showed that proteinase 3 early cleavage sites for PAR_1 are Ala^{36}-Thr^{37}, Pro^{48}-Asn^{49}, Val^{72}-Ser^{73}, Ala^{92}-Ser^{93}, and the late cleavage site is Pro^{54}-Phe^{55} (4). Furthermore, Sokolova *et al.* suggested in a recent review that proteinase 3 cleaves human PAR_1 at Ala^{36}-Thr^{37} and Val^{72}-Ser^{73} (29). Although there are differences, previous studies have agreed that the Val^{72}-Ser^{73} might be the earliest cleavage site for proteinase 3. We therefore altered that site by creating a mutation $A^{72}A^{73}$ in our N62QN75Q (named proteinase 3 mutant), and indeed the proteinase 3 almost immediately lost the ability to disarm the mutant receptor. As mentioned by Loew *et al.* there exists a late cleavage site between Pro^{54}-Phe^{55}, we therefore suggest that apart from the Val^{72}-Ser^{73} cleavage site there might exist relatively inefficient later cleavage events between Pro^{54}-Phe^{55}, and possibly at Pro^{48}-Asn^{49} (4). Thus there might be a possibility that if we expose PAR_1 to proteinase 3 for a greater length of time, proteinase 3 might disarm wt-$hPAR_1$. Indeed, we did notice that this phenomenon happened when we pre-incubated PAR_1 with

proteinase 3 for more than 3 min (data not shown). We have shown that in wt-$hPAR_1$ cells, proteinase 3 does not disarm the receptor immediately (within 1 min), however, after the removal of the glycans in Asn^{62} and Asn^{75} proteinase 3 immediately disarmed the glycosylation mutant receptor and inhibited thrombin-induced calcium mobilization. We therefore suggest that glycosylation of Asn^{62} and Asn^{75} together regulate $hPAR_1$ signalling to proteinase 3.

Our data also revealed that thermolysin disarms N62QN75Q with 30 fold better efficiency than wt-$hPAR_1$. One previous study in insect SF9 cells reported that thermolysin may represent an important mechanism of rapid receptor deactivation of the human thrombin receptor (34). Furthermore, like us, one previous study for PAR_1 in astrocytes found that treatment with thermolysin generated a thrombin-insensitive receptor, whereas the response to the activating peptide was not affected (35). In the literature, it is well established that the predicted thermolysin cleavage sites in PAR_1 are within the tethered ligand domain (SFLLR) at Phe^{43}-Leu^{44} and Leu^{44}-Leu^{45}, suggesting that thermolysin would be expected to remove the exodomain of PAR_1 and destroy the tethered ligand and thus disarm the receptor (16,36). Interestingly, in our study system, removing both of the glycosylation sequons (Asn^{62} and Asn^{75}) resulted in a receptor that was more efficiently disarmed by thermolysin, whereas removal of glycosylation at Asn^{62} sequon alone from the receptor had no observable effect on thermolysin disarming. However the N75Q did display increased disarming compared to wt-$hPAR_1$, thus suggesting that this sequon regulates PAR_1 disarming by thermolysin. Therefore, we predict that apart from the well established cleavage sites, there might be some other thermolysin cleavage sites in the N-terminus of PAR_1 especially in the region of the glycosylation site Asn^{75}. In theory, bacterial thermolysin cleaves peptide bonds amino-terminally to the hydrophobic residues leucine and isoleucine, with some specificity for phenylalanine and valine (36). Therefore we suggest that Leu^{71}- Val^{72} in PAR_1 may also be a potential thermolysin cleavage site, and it is very close to Asn^{75} site. When amputating the Asn^{75} glycan this potential thermolysin cleavage site (Leu^{71} -Val^{72}) will be more readily available for thermolysin cleavage.

In summary, $hPAR_1$ is a heavily glycosylated receptor and is important for cell surface expression, receptor stability and function. We show here for the first time that glycosylation in the N-terminus of $hPAR_1$ downstream of the tethered ligand (especially Asn^{75}) governs receptor disarming to trypsin, thermolysin, and the neutrophil proteinases elastase and proteinase 3, but not cathepsin G. Thus we concluded that *N*-linked glycosylation at N-terminus of $hPAR_1$ plays a vital role in regulating the susceptibility to proteinase disarming of the receptor.

REFERENCES

1. Ramachandran, R., and Hollenberg, M. D. (2008) *Br J Pharmacol* **153 Suppl 1**, S263-282
2. Macfarlane, S. R., Seatter, M. J., Kanke, T., Hunter, G. D., and Plevin, R. (2001) *Pharmacol Rev* **53**(2), 245-282
3. Hirano, K. (2007) *Arterioscler Thromb Vasc Biol* **27**(1), 27-36
4. Loew, D., Perrault, C., Morales, M., Moog, S., Ravanat, C., Schuhler, S., Arcone, R., Pietropaolo, C., Cazenave, J. P., van Dorsselaer, A., and Lanza, F. (2000) *Biochemistry* **39**(35), 10812-10822
5. Vouret-Craviari, V., Grall, D., Chambard, J. C., Rasmussen, U. B., Pouyssegur, J., and Van Obberghen-Schilling, E. (1995) *J Biol Chem* **270**(14), 8367-8372
6. Suidan, H. S., Bouvier, J., Schaerer, E., Stone, S. R., Monard, D., and Tschopp, J. (1994) *Proc Natl Acad Sci U S A* **91**(17), 8112-8116

7. Molino, M., Barnathan, E. S., Numerof, R., Clark, J., Dreyer, M., Cumashi, A., Hoxie, J. A., Schechter, N., Woolkalis, M., and Brass, L. F. (1997a) *J Biol Chem* **272**(7), 4043-4049
8. Suzuki, T., Moraes, T. J., Vachon, E., Ginzberg, H. H., Huang, T. T., Matthay, M. A., Hollenberg, M. D., Marshall, J., McCulloch, C. A., Abreu, M. T., Chow, C. W., and Downey, G. P. (2005) *Am J Respir Cell Mol Biol* **33**(3), 231-247
9. Nakayama, T., Hirano, K., Shintani, Y., Nishimura, J., Nakatsuka, A., Kuga, H., Takahashi, S., and Kanaide, H. (2003) *Br J Pharmacol* **138**(1), 121-130
10. Schechter, N. M., Brass, L. F., Lavker, R. M., and Jensen, P. J. (1998) *J Cell Physiol* **176**(2), 365-373
11. Ubl, J. J., Grishina, Z. V., Sukhomlin, T. K., Welte, T., Sedehizade, F., and Reiser, G. (2002) *Am J Physiol Lung Cell Mol Physiol* **282**(6), L1339-1348
12. Molino, M., Blanchard, N., Belmonte, E., Tarver, A. P., Abrams, C., Hoxie, J. A., Cerletti, C., and Brass, L. F. (1995) *J Biol Chem* **270**(19), 11168-11175
13. Renesto, P., Si-Tahar, M., Moniatte, M., Balloy, V., Van Dorsselaer, A., Pidard, D., and Chignard, M. (1997) *Blood* **89**(6), 1944-1953
14. Kuliopulos, A., Covic, L., Seeley, S. K., Sheridan, P. J., Helin, J., and Costello, C. E. (1999) *Biochemistry* **38**(14), 4572-4585
15. Norton, K. J., Scarborough, R. M., Kutok, J. L., Escobedo, M. A., Nannizzi, L., and Coller, B. S. (1993) *Blood* **82**(7), 2125-2136
16. Dery, O., Corvera, C. U., Steinhoff, M., and Bunnett, N. W. (1998) *Am J Physiol* **274**(6 Pt 1), C1429-1452
17. Shpacovitch, V., Feld, M., Bunnett, N. W., and Steinhoff, M. (2007) *Trends Immunol* **28**(12), 541-550
18. Hansen, K. K., Saifeddine, M., and Hollenberg, M. D. (2004) *Immunology* **112**(2), 183-190
19. Compton, S. J., Sandhu, S., Wijesuriya, S. J., and Hollenberg, M. D. (2002b) *Biochem J* **368**(Pt 2), 495-505
20. Compton, S. J., Renaux, B., Wijesuriya, S. J., and Hollenberg, M. D. (2001) *Br J Pharmacol* **134**(4), 705-718
21. Compton, S. J. (2003) *Drug Development Research* **59**, 350-354
22. Opdenakker, G., Rudd, P. M., Ponting, C. P., and Dwek, R. A. (1993) *Faseb J* **7**(14), 1330-1337
23. Wheatley, M., and Hawtin, S. R. (1999) *Hum Reprod Update* **5**(4), 356-364
24. Soto, A. G., and Trejo, J. (2010) *J Biol Chem* **285**(24), 18781-18793
25. Tordai, A., Brass, L. F., and Gelfand, E. W. (1995) *Biochem Biophys Res Commun* **206**(3), 857-862
26. Mize, G. J., Harris, J. E., Takayama, T. K., and Kulman, J. D. (2008) *Protein Expr Purif* **57**(2), 280-289
27. Brass, L. F., Vassallo, R. R., Jr., Belmonte, E., Ahuja, M., Cichowski, K., and Hoxie, J. A. (1992) *J Biol Chem* **267**(20), 13795-13798
28. Brass, L. F., Pizarro, S., Ahuja, M., Belmonte, E., Blanchard, N., Stadel, J. M., and Hoxie, J. A. (1994) *J Biol Chem* **269**(4), 2943-2952
29. Sokolova, E., and Reiser, G. (2007) *Pharmacol Ther* **115**(1), 70-83
30. Ramachandran, R., Sadofsky, L. R., Xiao, Y., Botham, A., Cowen, M., Morice, A. H., and Compton, S. J. (2007) *Am J Physiol Lung Cell Mol Physiol* **292**(3), L788-798
31. Sambrano, G. R., Huang, W., Faruqi, T., Mahrus, S., Craik, C., and Coughlin, S. R. (2000) *J Biol Chem* **275**(10), 6819-6823

32. Rao, N. V., Wehner, N. G., Marshall, B. C., Gray, W. R., Gray, B. H., and Hoidal, J. R. (1991a) *J Biol Chem* **266**(15), 9540-9548
33. Uehara, A., Sugawara, S., Muramoto, K., and Takada, H. (2002) *J Immunol* **169**(8), 4594-4603
34. Chen, X., Earley, K., Luo, W., Lin, S. H., and Schilling, W. P. (1996) *Biochem J* **314 (Pt 2)**, 603-611
35. Ubl, J. J., Sergeeva, M., and Reiser, G. (2000) *J Physiol* **525 Pt 2**, 319-330
36. Hamilton, J. R., Chow, J. M., and Cocks, T. M. (1999) *Br J Pharmacol* **127**(3), 617-622

FOOTNOTES

Abbreviations used are: KNRK, Kirsten murine sarcoma virus transformed rat kidney cells; CHO, Chinese hamster ovary cells; PCR, polymerase chain reaction; POMC, pro-opiomelanocortin; eYFP, enhanced yellow fluorescent protein; $hPAR_1$, human proteinase activated receptor-1; $hPAR_1E$, human proteinase activated receptor-1 with eYFP tag; PAR_1-AP, PAR_1 activating peptide; TF, TFLLR-NH_2; TH, thrombin; THE, thermolysin; PR3, proteinase 3; CG, cathepsin G; ELA, human leukocyte elastase;

FIGURE LEGENDS

Fig. 1. Representative model of $hPAR_1$ displaying the five potential *N*-linked glycosylation sequons and potential proteinase cleavage sites at the extracellular N-terminus. Three sequons are located on the receptor N-terminus ($N^{35}A^{36}T^{37}$, $N^{62}E^{63}S^{64}$, $N^{75}K^{76}S^{77}$) and two are located within extracellular loop 2 (ECL2; $N^{250}I^{251}T^{254}$, $N^{259}E^{260}T^{261}$). Of the sequons at the N-terminus, one ($N^{35}A^{36}T^{37}$) is located N-terminal of the cleavage/activation site (R^{41}/S^{42}FLLR) and the remaining two ($N^{62}E^{63}S^{64}$, $N^{75}K^{76}S^{77}$) are located downstream of the cleavage/activation site. The disulphide bridge is shown by the two cysteines (C-C). The red arrows indicate the preferential cleavage site for each proteinase. TH, thrombin; TRY, trypsin; THE, thermolysin; PR3, proteinase 3; CG, cathepsin G; ELA, elastase. [Adapted from (4,12,13,29)].

Fig. 2. Cell-surface expression of wt-$hPAR_1$(WT) and glycosylation-deficient mutant $hPAR_1$ receptor in KNRK cells assessed by FACs. Cells at approx 90% confluence were harvested and incubated with the ATAP-2 antibody before incubation with an anti-mouse FITC-conjugated antibody. Results are expressed as a percentage of the median fluorescence obtained with wt-$hPAR_1$ cells. The bars represent mean ± SEM of measurements for three independent experiments. The overall comparsion showed that there were significant differences between 10 groups ($p<0.0001$). Tukey's Multiple Comparison Test indicated that the cell-surface expression of all the mutant receptors were significantly different from wt-$hPAR_1$ ($p<0.001$).

Fig. 3. Confocal microscopy for wt-$hPAR_1E$ and glycosylation-deficient mutants in KNRK cells. eYFP tagged PAR_1 expressing KNRK cells were grown on coverslips before fixing and permeabilising. Cells were stained with propidium iodide prior to visualising. eYFP is visualised here in green and propidium iodide in red. I: cell surface expression, II: internal receptor expression. Green bar on the right of each panel stands for 10µm scale bar. A, EV; B, wt-$hPAR_1E$; C, N35Q$hPAR_1E$; D, N62QN75Q$hPAR_1E$; E, N250N259Q$hPAR_1E$; F, N35-259Q$hPAR_1E$. The images are representative for four independent experiments.

Fig. 4. Western blot analysis for wild-type and glycosylation-deficient mutant $hPAR_1$. (A) Immunoprecipitates from KNRK cell lines expressing HA.11-tagged $hPAR_1$ with the potential *N*-linked glycosylation sequons removed, were analysed by SDS/PAGE (10% gel)

and immunoblotted using HA.11 monoclonal antibody. Lane 1, EV; Lane 2, WT-hPAR_1E; Lane 3, N62QhPAR_1E; Lane 4, N62QN75QhPAR_1E; Lane 5, N35QN62QN75QhPAR_1E; Lane 6, N250N259QhPAR_1E; Lane 7, N35-259QhPAR_1E. (B) Protein samples of hPAR_1E transfected CHO (Pro5 and Lec2) cell lines were immunoprecipitated by HA.11 immunoprecipitation and were analysed by SDS/PAGE (10% gel) and immunoblotted using a monoclonal HA.11 antibody. Lane 1, Pro5; Lane 2, Pro5-PAR_1E; Lane 3, Lec2; Lane 4, Lec2-PAR_1E. GD indicates glycosylated dimer; NGD, nonglycosylated dimer; GM, glycosylated monomer; NGM, nonglycosylated or minimally glycosylated monomer. M indicated nonglycosylated or minimally glycosylated monomer; D, PAR_1 dimer. M.M., molecular mass. Results are representative of three separate experiments.

Fig. 5. Cell surface expression and calcium signalling analysis of WT-M and N62QN75Q. (A) Comparison of WT-M and glycosylation-deficient mutant N62QN75Q KNRK cell-surface expression. Cells at approx 90% confluence were harvested and incubated with the ATAP-2 antibody before incubation with an anti-mouse FITC-conjugated antibody. Cell surface expression was assessed by FACS analysis. Results are expressed as a percentage of the median fluorescence obtained with WT cells. (B), (C), (D) Calcium signalling in the WT-M and glycosylation mutant N62QN75Q in response to TFLLR-NH_2, thrombin and trypsin. Results are expressed as the means ± SEM of at least four independent experiments.

Fig. 6. (A) Analysis of trypsin disarming in WT-M and N62QN75Q. Calcium imaging of fluo-3 loaded cells was used to assess 100 μM TFLLR-NH_2 responses following trypsin and then 5 nM thrombin challenge in wt-hPAR_1 and hPAR_1(N62QN75Q) transfected KNRK cells. The cellular response to TFLLR-NH_2 after the addition of thrombin but without pre-treatment with trypsin is used as a % control. (B) Analysis of trypsin disarming in N62Q. hPAR_1(N62Q) transfected KNRK cells calcium signalling response following the addition of 100 nM trypsin, 5 nM thrombin, and 100 μM TFLLR-NH_2 and then 2 μM A23187. (C) Analysis of trypsin disarming in N75Q. hPAR_1(N75Q) transfected KNRK cells calcium signalling response following the addition of 100 nM trypsin, 5 nM thrombin, 100 μM TFLLR-NH_2 and then 2 μM A23187. TRY, Trypsin; TH, thrombin; TF, TFLLR-NH_2. The data sets are expressed as mean ± SEM from three separate experiments.

Fig. 7. Analysis of WT-M and hPAR_1(N62QN75Q) calcium signalling following proteinase stimuli. WT-M and N62QN75Q in KNRK cells were challenged by (A) the addition of elastase; (B) the addition of cathepsin G; (C) the addition of proteinase 3; (D) the addition of thermolysin followed by the addition of 5 nM thrombin, and finally the addition of 2 μM A23187. Results are expressed as mean ± SEM from at least three independent experiments.

Fig. 8. Molecular evidence that cathepsin G and proteinase 3 disarm hPAR_1(N62QN75Q). (A) CG mutant and (B) proteinase 3 mutant cells loaded with Fluo-3 were stimulated by the addition of either 100 nM cathepsin G, or 300 nM proteinase 3 for 2mins and then challenged with 5 nM thrombin, followed by 100 μM TFLLR-NH_2 and then 2 μM calcium ionophore (A23187). TH, thrombin; CG, cathepsin G; PR3, proteinase 3. Results are expressed as the mean ± SEM of at least two independent experiments.

Fig. 9. Analysis of hPAR_1(N62Q) and hPAR_1(N75Q) calcium signalling following proteinase stimuli. (A) N62Q and (B) N75Q cells loaded with Fluo-3 were stimulated by the addition of either 50 nM thermolysin, 1.5 nM elastase, 100 nM cathepsin G, or 300 nM proteinase 3 for 2mins and then challenged with 5 nM thrombin, followed by 100 μM TFLLR-NH_2 and then 2 μM A23187. TRY, Trypsin; TH, thrombin; TF, TFLLR-NH_2; THE, thermolysin; ELA, elastase; CG, cathepsin G; PR3, proteinase 3. Results are expressed as the mean ± SEM of at least three independent experiments.

Table 1. Table showing KNRK and CHO fibroblast (Pro5 and Lec2) permanently expressing (A) wild type or (B) *N*-linked glycosylation mutant $hPAR_1$ cell clones generated for this study. In order to obtain permanent receptor expressing cell lines, cells expressing high levels of $hPAR_1$ were isolated by FACS using the ATAP-2 anti-PAR_1 antibody. The glycosylation mutants were named with an N followed by a number related to the relative position of the potential glycosylation site and a Q. The alanine mutations were created at amino acid position Phe^{55}-Trp^{56} or Val^{72}-Ser^{73} of N62QN75Q to generate cathepsin G mutant (F55AW56A) or proteinase 3 mutant (V72AS73A).

(A)

Name of Clones	Receptor cell surface expression level	Cell Type
WT	Maximum level of wt-$hPAR_1$ cell surface expression	KNRK & CHO
WT-$hPAR_1$E	Maximum level of wt-$hPAR_1$E cell surface expression	KNRK & CHO
WT-H	Higher level of wt-$hPAR_1$ cell surface expression	KNRK
WT-M	Medium level of wt-$hPAR_1$ cell surface expression	KNRK
WT-L	Low level wt-$hPAR_1$ cell surface expression	KNRK

(B)

Name of Clones	Consensus Sequence(s) Disrupted	Cell Type
N35Q	Asn^{35}	KNRK
N62Q	Asn^{62}	KNRK
N75Q	Asn^{75}	KNRK
N250Q	Asn^{250}	KNRK
N259Q	Asn^{259}	KNRK
N62QN75Q	Asn^{62} and Asn^{75}	KNRK
N35QN62QN75Q	Asn^{35}, Asn^{62} and Asn^{75}	KNRK
N250QN259Q	Asn^{250} and Asn^{259}	KNRK
N35-259Q	Asn^{35}, Asn^{62}, Asn^{75}, Asn^{250} and Asn^{259}	KNRK
N35Q $hPAR_1$E	Asn^{35}	KNRK
N62QN75Q $hPAR_1$E	Asn^{62} and Asn^{75}	KNRK
N250QN259Q$hPAR_1$E	Asn^{250} and Asn^{259}	KNRK
N35-259Q $hPAR_1$E	Asn^{35}, Asn^{62}, Asn^{75}, Asn^{250} and Asn^{259}	KNRK
Cathepsin G mutant	Asn^{62} , Asn^{75}, Phe^{55} and Trp^{56}	KNRK
Proteinase 3 mutant	Asn^{62}, Asn^{75}, Val^{72} and Ser^{73}	KNRK

Table 2. EC_{50} values for N-terminal glycosylation-deficient mutant $hPAR_1$ and their respective matching cell surface expression of wt-$hPAR_1$ agonist concentration effect curves. Cell clones with matched receptor expression assessed by FACS analysis were selected for functional studies. Where it was not possible to match receptor expression between the wt-$hPAR_1$ cell line and a cell line expressing a mutant glycosylation receptor, the WT, WT-H, WT-M and WT-L with different cell confluence in order to reduce receptor expression were used and thus match the cell surface expression of the mutant cell line. Reduced receptor cell surface expression of the WT-H, WT-M and WT-L cell lines were confirmed by using FACS analysis.

Cell lines with matched receptor expression	**EC_{50}**		
	TFLLR [µM]	**Thrombin [nM]**	**Trypsin [nM]**
WT-H	17	0.14	33
N35Q	16	0.2	43
WT-L	27	0.2	39
N62Q	29	0.4	43
N75Q	31	0.2	41
WT-M	22	0.12	26
N62QN75Q	30	0.3	**42**

Figure 1.

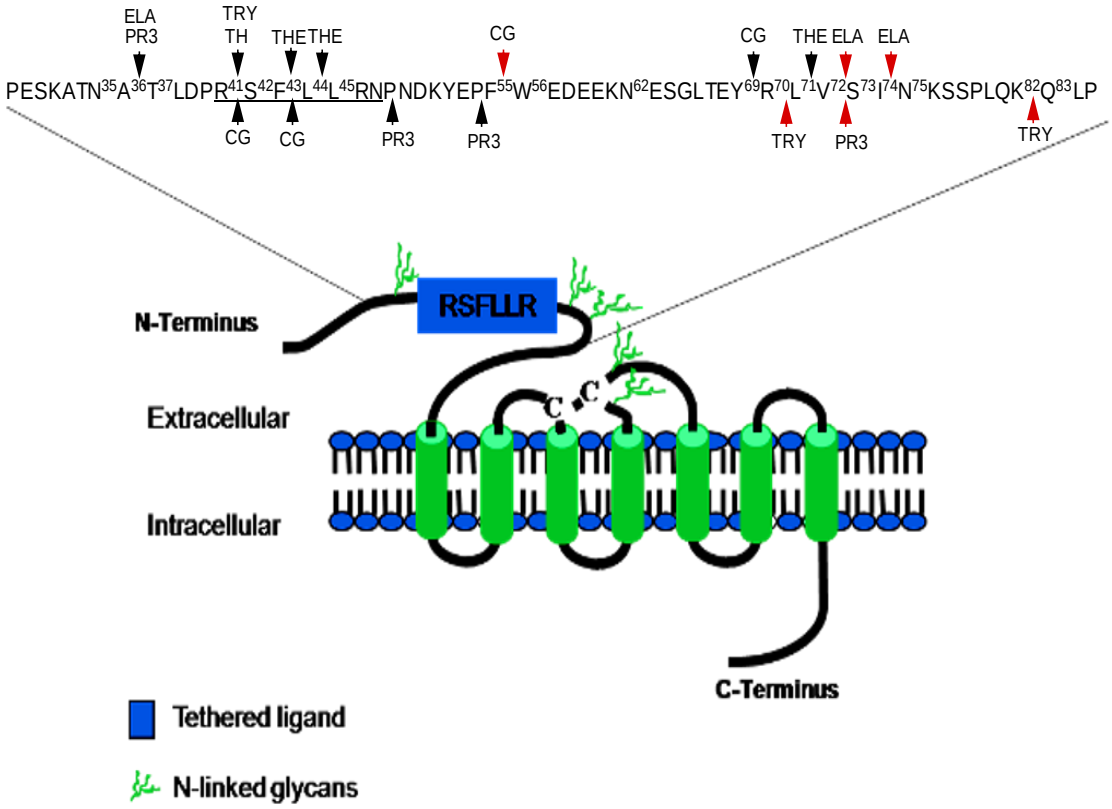
ELA
PR3
TRY
TH
THE THE
CG
CG
THE ELA
ELA
PESKATN35A36T37LDPR41S42F43L44L45RNPNDKYEPF55W56EDEEKN62ESGLTEY69R70L71V72S73I74N75KSSPLQK82Q83LP
CG
CG
PR3
PR3
TRY
PR3
TRY
N-Terminus
RSFLLR
Extracellular
Intracellular
C-Terminus
Tethered ligand
N-linked glycans

Figure 2.

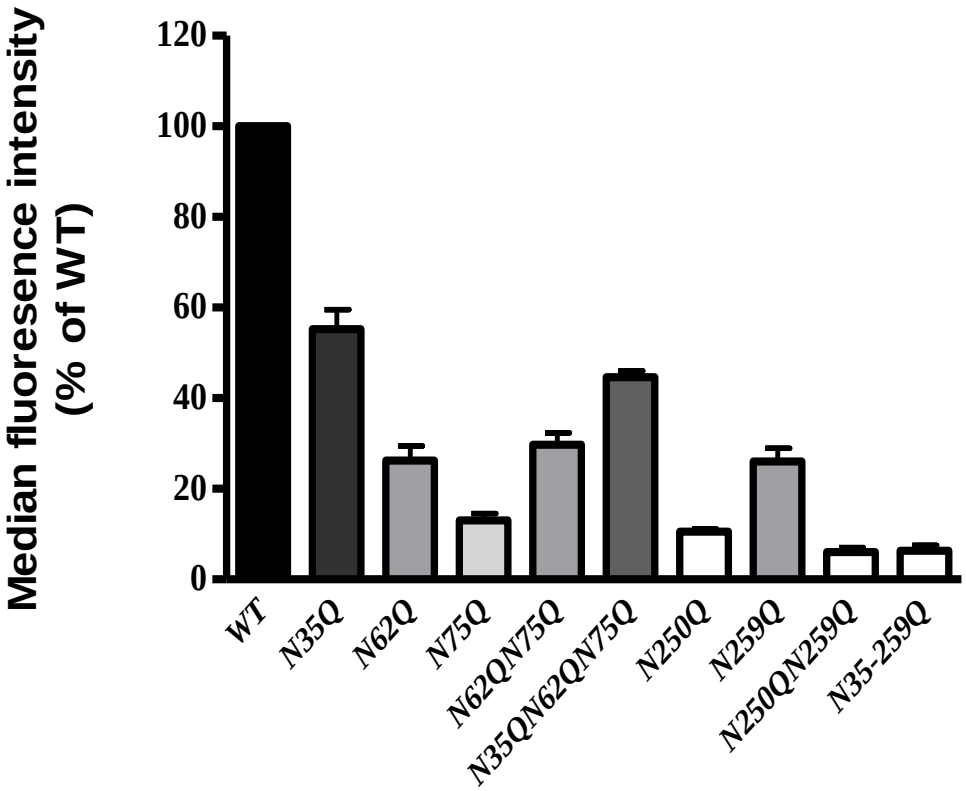
Median fluoresence intensity
(% of WT)
120
100
80
60
40
20
0
WT
N35Q
N62Q
N75Q
N62QN75Q
N35QN62QN75Q
N250Q
N259Q
N250QN259Q
N35-259Q

Figure 3.

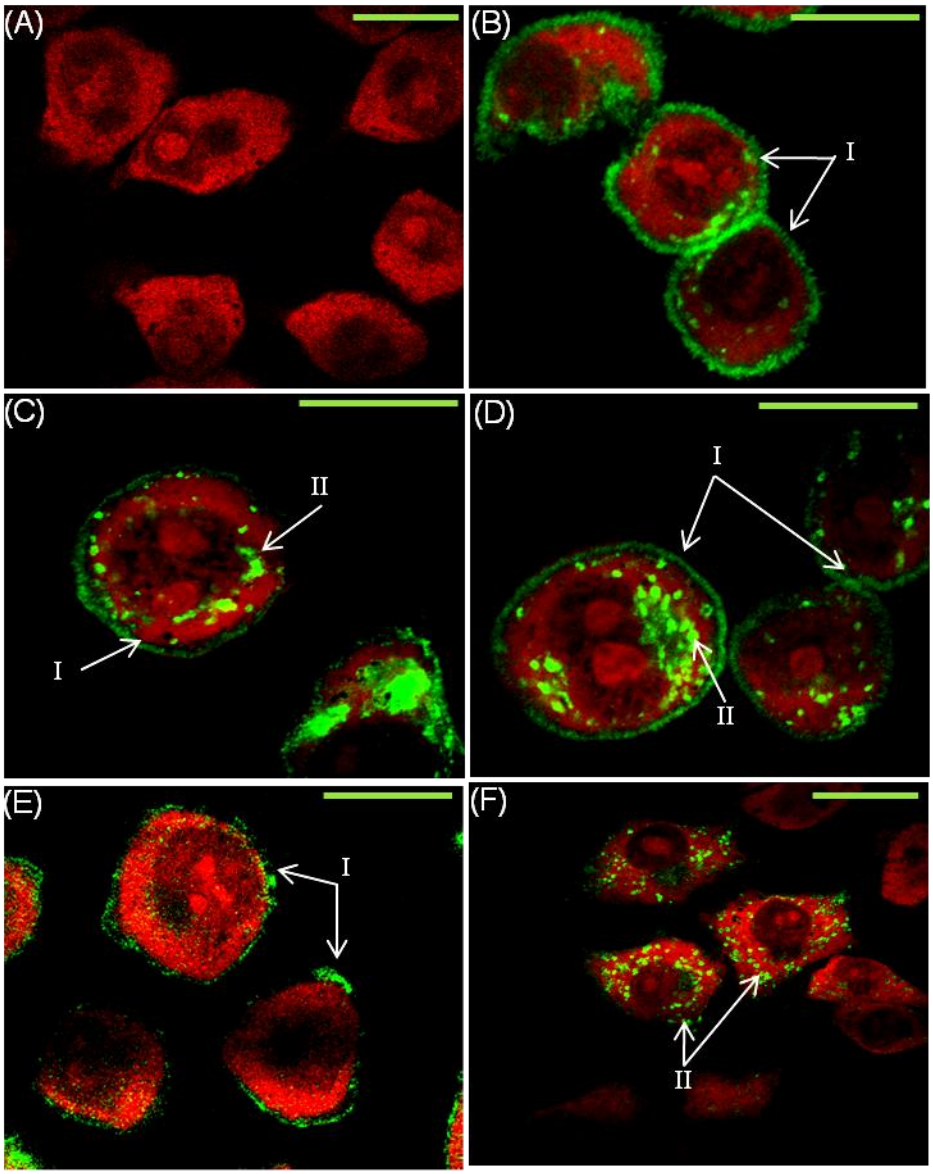

Figure 4.

(A)

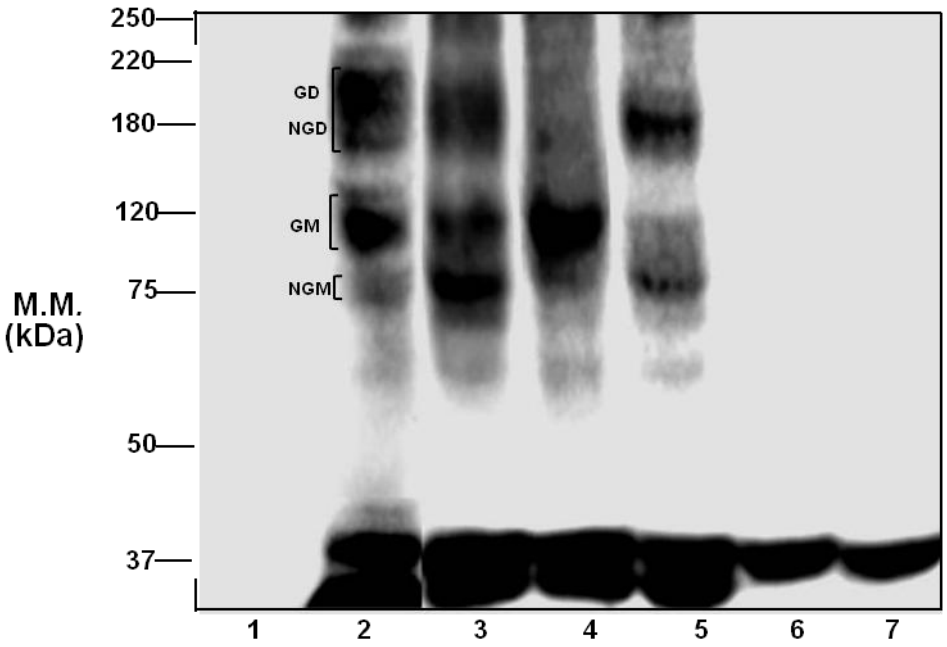
250
220
180
120
75
50
37
M.M.
(kDa)
GD
NGD
GM
NGM
1
2
3
4
5
6
7

(B)

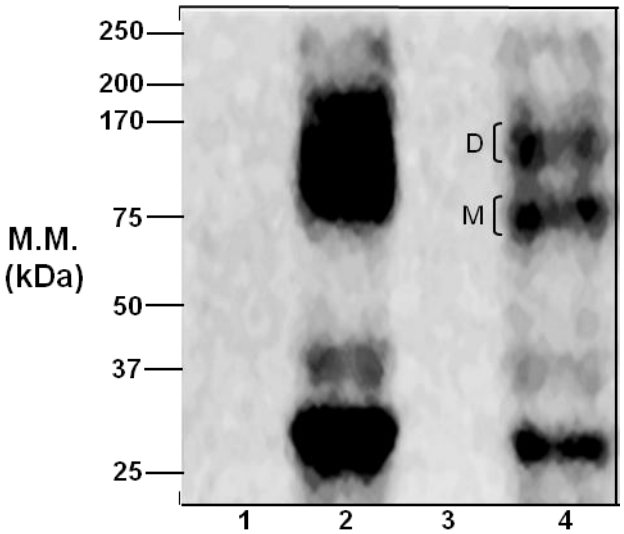
250
200
170
75
50
37
25
M.M.
(kDa)
D
M
1
2
3
4

Figure 5.

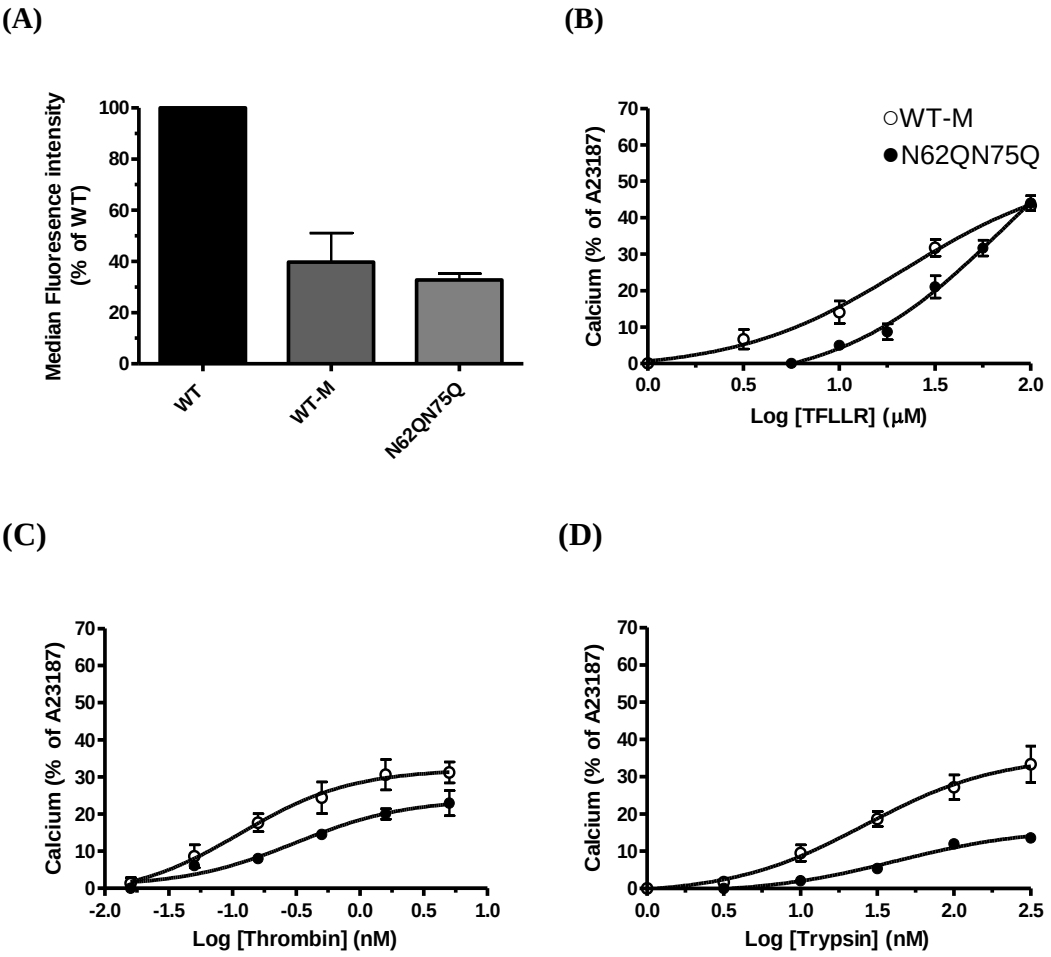
(A)
(B)
Median Fluoresence intensity (% of WT)
100
80
60
40
20
0
WT
WT-M
N62QN75Q
○WT-M
●N62QN75Q
Calcium (% of A23187)
70
60
50
40
30
20
10
0
0.0
0.5
1.0
1.5
2.0
Log [TFLLR] (μM)
(C)
(D)
Calcium (% of A23187)
-2.0
-1.5
-1.0
-0.5
0.0
0.5
1.0
Log [Thrombin] (nM)
Calcium (% of A23187)
0.0
0.5
1.0
1.5
2.0
2.5
Log [Trypsin] (nM)

Figure 6.

(A)

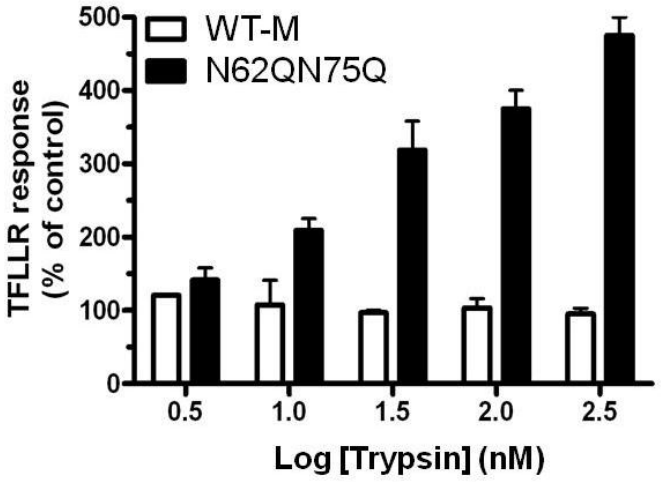
WT-M
N62QN75Q
TFLLR response
(% of control)
500
400
300
200
100
0
0.5
1.0
1.5
2.0
2.5
Log [Trypsin] (nM)

(B)

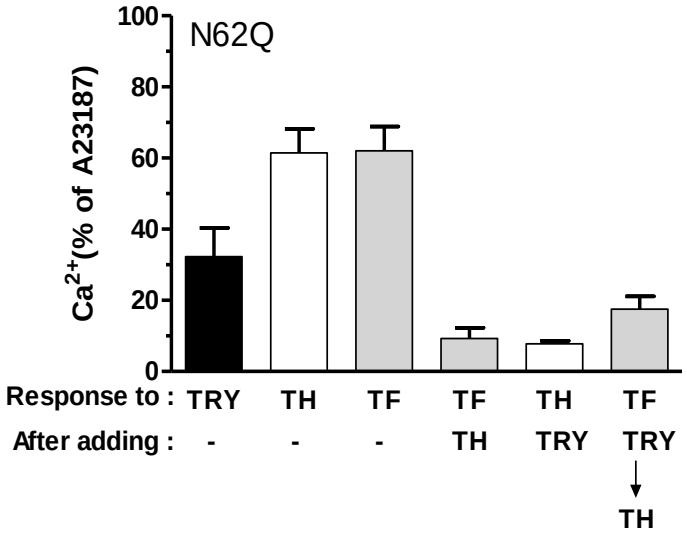
N62Q
Ca2+(% of A23187)
100
80
60
40
20
0
Response to : TRY TH TF TF TH TF
After adding : - - - TH TRY TRY
TH

(C)

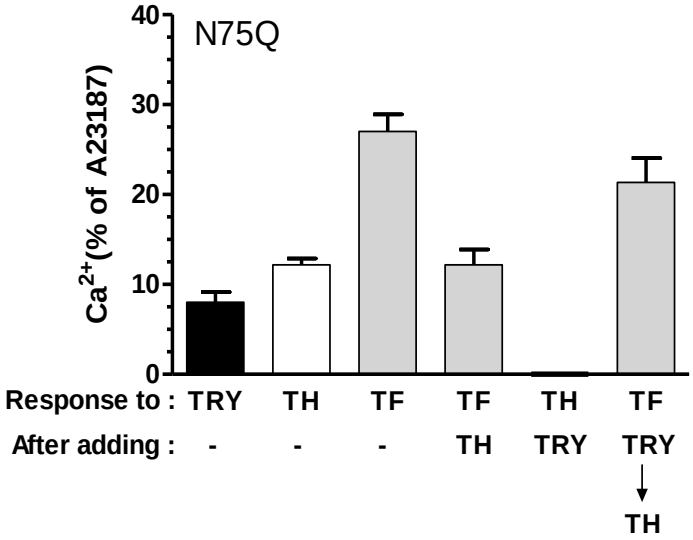
N75Q
Ca2+(% of A23187)
40
30
20
10
0
Response to : TRY TH TF TF TH TF
After adding : - - - TH TRY TRY
TH

Figure 7.

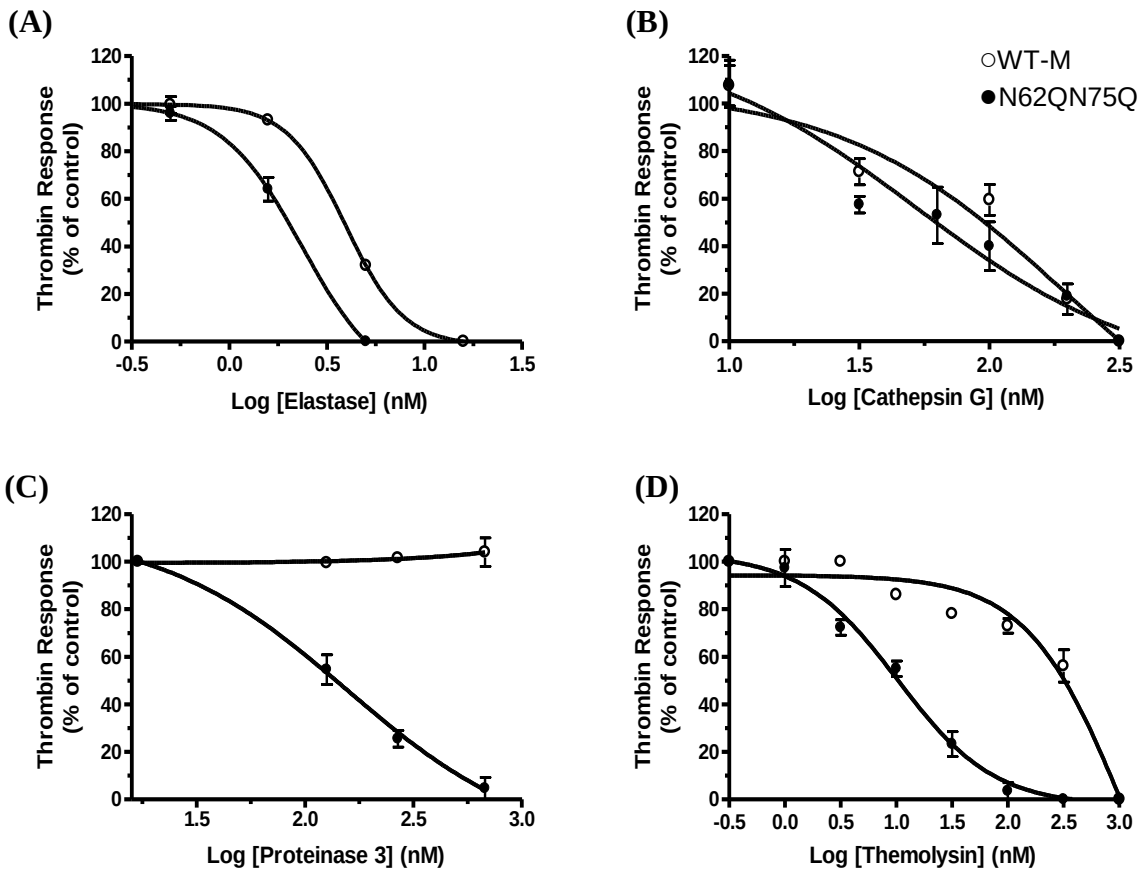
(A)
Thrombin Response (% of control)
Log [Elastase] (nM)
(B)
○WT-M
●N62QN75Q
Thrombin Response (% of control)
Log [Cathepsin G] (nM)
(C)
Thrombin Response (% of control)
Log [Proteinase 3] (nM)
(D)
Thrombin Response (% of control)
Log [Themolysin] (nM)

Figure 8.

(A)

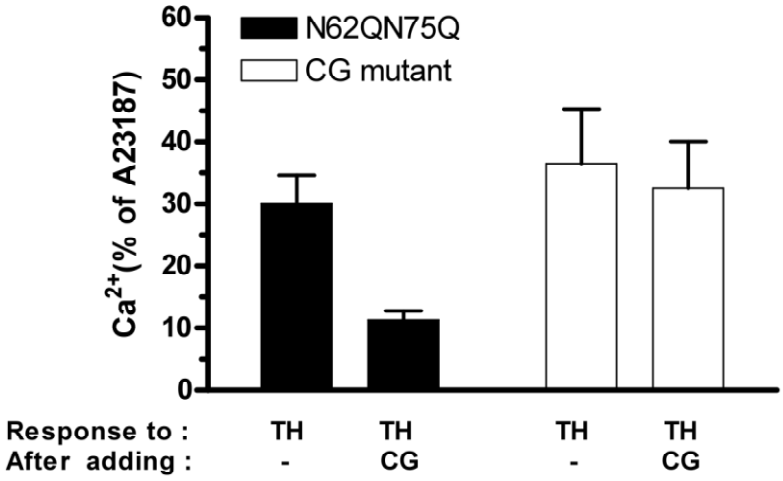
N62QN75Q
CG mutant
Ca2+(% of A23187)
60
50
40
30
20
10
0
Response to : TH TH TH TH
After adding : - CG - CG

(B)

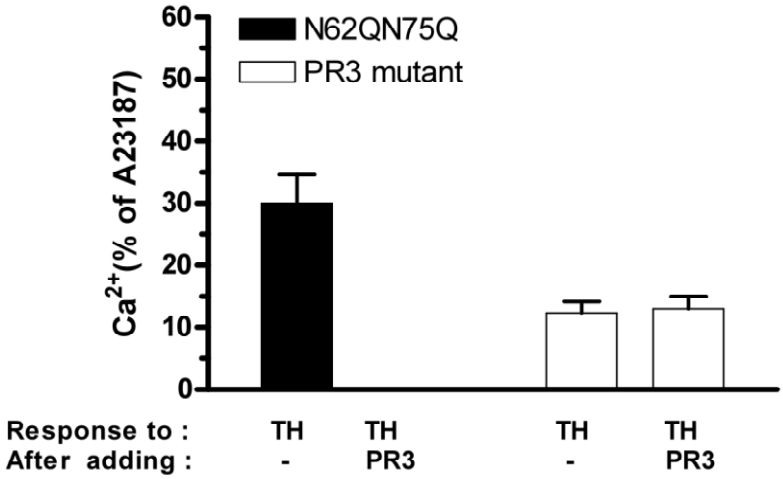
N62QN75Q
PR3 mutant
Ca2+(% of A23187)
60
50
40
30
20
10
0
Response to : TH TH TH TH
After adding : - PR3 - PR3

Figure 9.

(A)

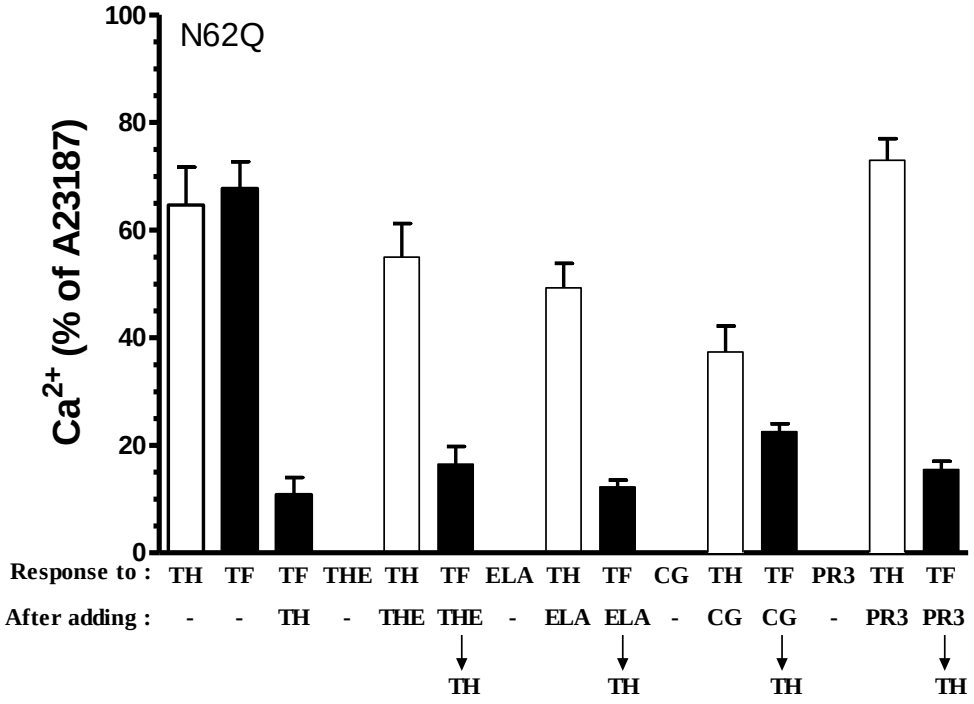
N62Q
Ca2+ (% of A23187)
100
80
60
40
20
0
Response to : TH TF TF THE TH TF ELA TH TF CG TH TF PR3 TH TF
After adding : - - TH - THE THE - ELA ELA - CG CG - PR3 PR3
TH TH TH TH

(B)

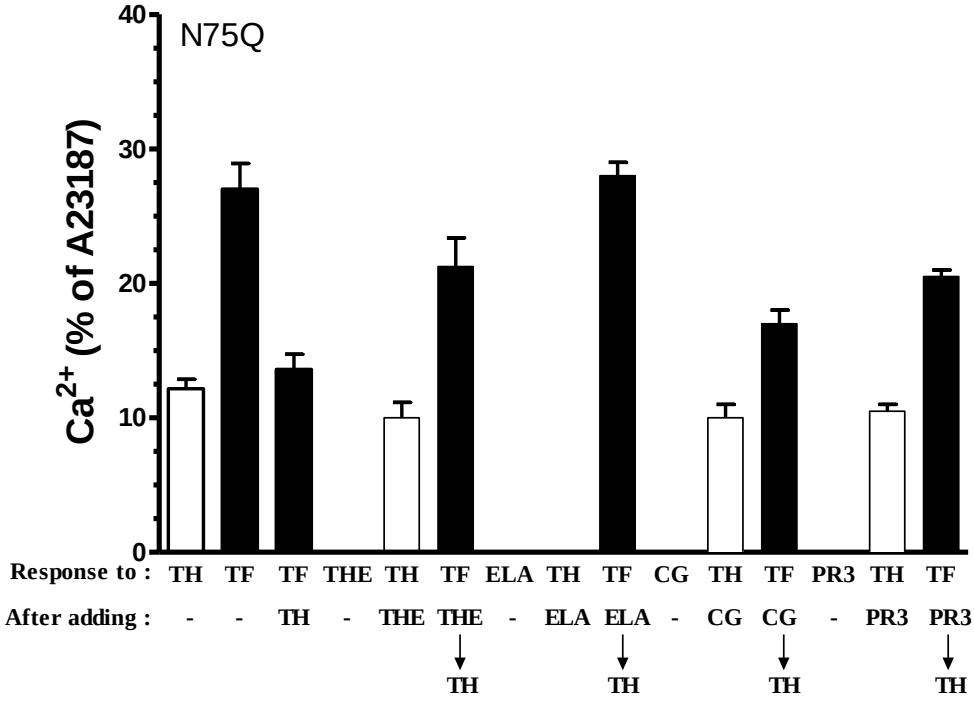
N75Q
Ca2+ (% of A23187)
40
30
20
10
0
Response to : TH TF TF THE TH TF ELA TH TF CG TH TF PR3 TH TF
After adding : - - TH - THE THE - ELA ELA - CG CG - PR3 PR3
TH TH TH TH